CHAPTER 2. SFERICS MEASUREMENTS AND CORRELATION ANALYSIS

Sferics noise contaminating TEM measurements is an unwanted variation of signal with time in the sensor response. It has been shown that a reduction in sferics noise by a factor of 5 to 10 in an area where the sferics noise predominates over variations in background geological signal will increase the detectable target depth by 50 to 80% (Buselli and Cameron, 1995). Such an improvement can be achievable in areas of northern Australia where summer sferics activity is higher by a factor of about 50 to 100 than the sferics activity in winter in southern region of Australia.

In order to understand the characteristics of sferics noise and develop methods of reducing sferics noise, three-component sferics correlation measurements were carried out with various separations between two receivers. The correlation between orthogonal components of the sferics noise and the spatial correlation of sferics noise in both horizontal and vertical planes were investigated to establish the efficacy of using multiple remote or local reference receivers for EM noise reduction.

2.1 Instrumentation for sferics correlation measurements

2.1.1 High-frequency sferics measurements

The arrangement of instruments and equipment used for the measurement of the correlation of high-frequency (> ~ 5 kHz) sferics noise is shown in Figure 2.1. The equipment is duplicated at two stations and measurements are made with these two stations separated by various distances. At each station, three orthogonal components of the sferics noise are detected with a three-component roving vector receiver, RVR-3C, normally used for measurements with SIROTEM. The signals pass

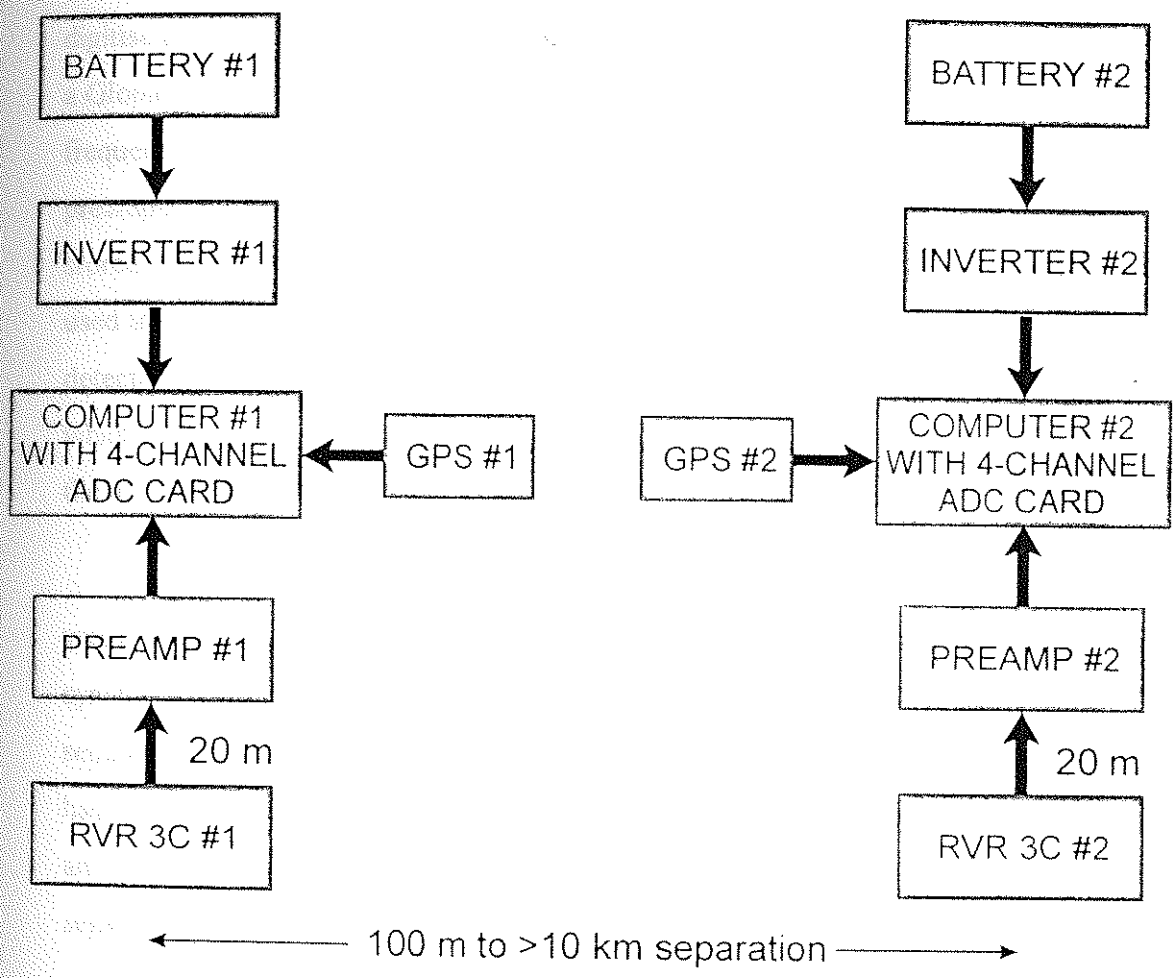

Figure 2.1 Two-station data acquisition system for high-frequency sferics.

through a three-channel preamplifier, each of which enables the choice of three gain settings of 1, 10 and 100. Saturation of each preamplifier by a sferics pulse is indicated by a flashing light on each preamplifier. The gain is chosen such that the number of sferics saturating the preamplifiers is minimal.

Three channels of a 12-bit analogue-to-digital converter (ADC) are used to digitise the preamplified signals simultaneously. One-second time marks derived from a Global Positioning System (GPS) are placed on the fourth ADC channel. For high-frequency sferics, an anti-aliasing filter of 100 kHz is placed at the input of the preamplifiers. Digitisation is carried out at a sampling rate of 250 kHz. The data are stored on a 2 Giga-byte hard disc of a Compaq PC. DC voltage from an inverter is used to power the computer to avoid generation of 50 Hz noise, which could be detected by the noise system. A data acquisition program was written using Labview, which is a graphical programming language, and a Watcom C++ compiler to create the interface library between the data acquisition program and GPS unit.

Until December 1994, synchronisation of measurements at the two stations was provided by a wire link between the two stations. Since the length of a synchronisation cable which could conveniently be laid out was 1 km, the maximum separation of the two stations was limited to this distance. Since then, synchronisation has been derived from the one-second pulses provided by GPS units at each station, and this method places no limit on the station separation. To date, the maximum separation at which correlation measurements have been made is 11 km.

2.1.2 Low-frequency sferics measurements

The results of sferics measurements with an RVR-3C demonstrate that significant power from sferics is not detected with this sensor below a frequency in the range of 2 to 5 kHz (see Section 2.5.1). Calculations (see Appendix 1) show that for each component of the noise, a coil or loop area larger than the passive area of the

corresponding coil of the RVR-3C is required to detect sferics below 2 kHz. For measurements of sferics in the frequency range of 1 Hz to 1 kHz, each RVR-3C shown in Figure 2.1 is replaced by two separate horizontal-axis induction coils (called Drovers) to measure the horizontal (X and Y) components of the noise, and a two-turn 100-m loop to measure the vertical (Z) component.

Low-frequency measurements of each component are made with a 10 kHz anti-aliasing filter placed at the input of the preamplifiers, and a 1 kHz filter at the output of the preamplifier. The three components of the noise are simultaneously digitised at a sampling rate of 10 kHz.

2.2 Sferics count rates and daily variation of sferics activity

In order to compare sferics activities at four field sites in Australia (Figure 2.2): Ku-Ring-Gai National Park near Sydney, Mt Isa, Koolpinyah near Darwin, and Parkes, the noise data measured at each place in the afternoon was used to count sferics pulses. All count rates shown in Table 2.1 were calculated with a threshold of 20% larger than any low-frequency variations in the background EM noise level, and with a deadtime of 1 ms after the occurrence of any sferics pulse. For example, the count rate of 253 sferics pulses per sec of Darwin data measured in 1983 was obtained with a threshold of 0.2 mV (background noise level is ~0.17 mV). The sferics activity of the 1983 Darwin data is 2 and 5 time higher than Darwin data and Ku-Ring-Gai data, respectively, measured in February 1994. Comparing all sferics count rates of Ku-Ring-Gai data, the sferics activity in summer is more than 4 time higher than that in autumn.

Figure 2.3 shows daily variations of the three-component sferics count rates at Ku-Ring-Gai National Park. Sferics noise data were measured from 11:00 AM of the 28th to 11:00 AM of the 29th of December 1994 with an interval of 30 min between each measurement. The record length of each noise data is 5 sec. The minimum sferics

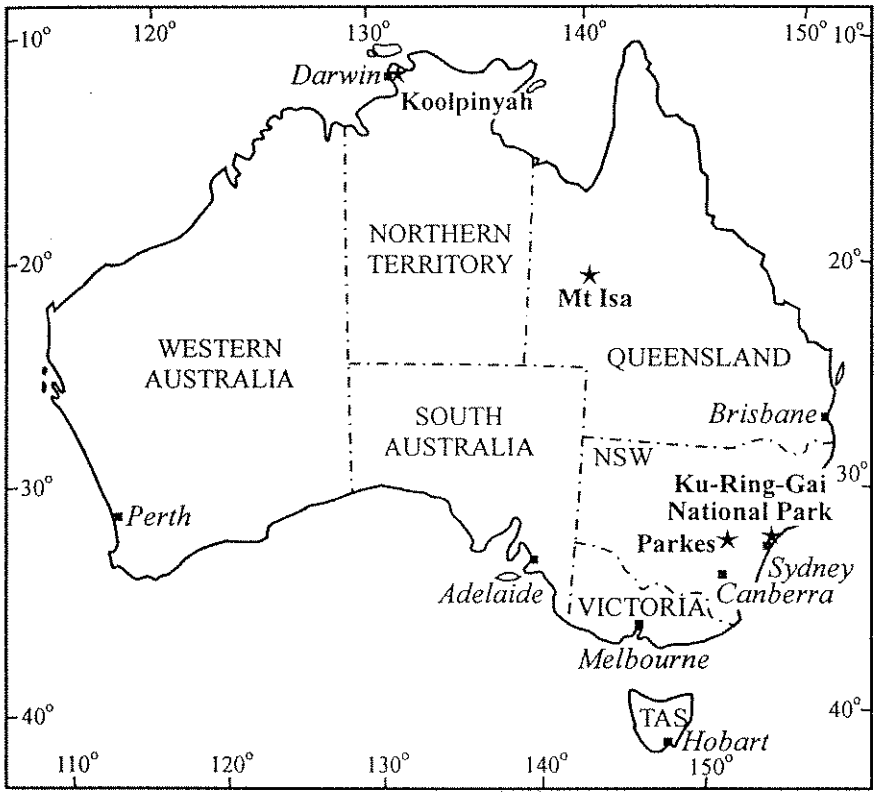

Figure 2.2 Locality map of sites where sferics measurements have been made in Australia.

Table 2.1 Sferics count rates at four sites in Australia as shown.

Survey Site	Date	Number of sferics [pulses per sec]	Total record length [sec]	Approximate recording time
Darwin	Feb. 1983	253	82	4:00 PM
	Dec. 1994	123	23	2:40 PM
Mt. Isa	Mar. 1994	21	28	2:50 PM
Ku-Ring-Gai National Park	Feb. 1994	52	20	2:40 PM
	Mar. 1994	23	21	2:50 PM
	Apr. 1994	16	7	3:00 PM
	Dec. 1994	71	20	2:00 PM
	Mar. 1995	22	20	3:50 PM
Parkes	Aug. 1995	6	25	3:30 PM

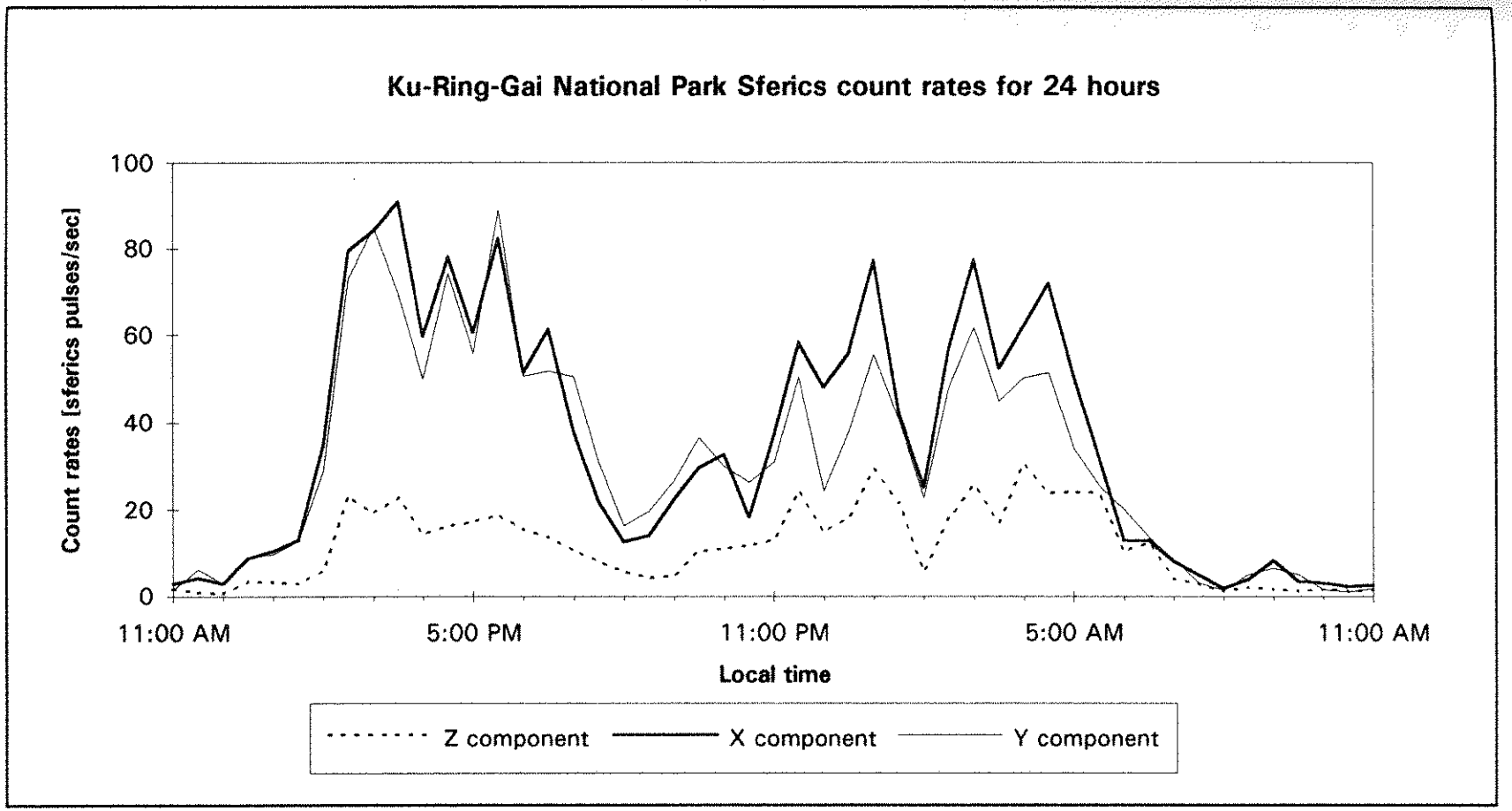

Figure 2.3 One-day monitoring of high-frequency sferics at Ku-Ring-Gai National Park in the 28th to 29th of December 1994.

activity periods occur from 6:30 AM to 1:30 PM and from 6:30 to 10:30 PM. The sferics count rates during these minimum activity periods are about 3 to 9 times smaller than those during maximum activity periods.

2.3 Measures of correlation

Sferics data collected simultaneously at two stations may be processed in various ways to present them in a form suitable for providing an overview of their correlation. The methods investigated so far are discussed in this Section, and the mathematical expressions for the functions used to measure correlation are given in the Appendix 2.

2.3.1 Cross-correlation function

One way of examining the correlation between two time series, $g(t)$ and $h(t)$, is to calculate their cross-correlation function, $\phi_{gh}(\tau)$. The degree of correlation between the two time series is obtained by shifting one time series relative to the other series by a time, τ, and summing the products of corresponding samples of the two series. This procedure is repeated for a range of values of τ. To ensure that the values of $\phi_{gh}(\tau)$ lie between -1 and 1, they are divided by the square root of a normalising function, which is the product of the sum of the squares of the samples of each series.

Thus, if $g(t) = h(t)$ for all corresponding samples of the two series with a given delay τ between them, the two series are perfectly correlated at this value of τ and $\phi_{gh}(\tau)$ has a value of 1. If $g(t) = -h(t)$ for all samples, then at this value of τ the value of $\phi_{gh}(\tau)$ is -1, and the two time series are anti-correlated.

The mathematical expression for $\phi_{gh}(\tau)$ is given in Equation A2.1 of the Appendix 2.

2.3.2 Cross-power and cross-phase spectra

The cross-correlation function may have a complex form when the time series contain more than one frequency component. The main frequency components present in the time series may be found by producing the power spectrum, $G(f)$ and $H(f)$ of the time series, $g(t)$ and $h(t)$, respectively. Both $G(f)$ and $H(f)$ are obtained by applying the fast Fourier Transform (FFT) to the corresponding time series and squaring the result.

To separate the degree of correlation at different frequencies, both cross-power and cross-phase spectra are derived from the power spectrum of each time series. The cross-power spectrum, $S_{gh}(f)$ is essentially the product of the power spectra, $G(f)$ and $H(f)$ of the two time series. The cross-phase spectrum, $\phi_{gh}(f)$ is the value of the angle having a tangent ratio given by the ratio of the imaginary to the real part of the cross-power spectrum.

When the plot of $\phi_{gh}(f)$ as a function of frequency, f, is a straight line, it can be shown that the slope of this line is the time shift, τ between the two time series. A value of τ can be obtained more accurately by this method than it can be from the cross-correlation function. All plots of the cross-phase spectrum in this report are accompanied by a value of τ deduced from that spectrum.

Mathematical expressions for the power spectra, cross-power spectrum and cross-phase spectrum of two time series, and the time shift between two time series are given in Equations A2.2, A2.3, A2.4, A2.5 and A2.14 of the Appendix 2.

2.3.3 Squared coherency spectrum

To obtain values in the range of 0 to 1 for the cross-power spectrum, the square of the cross-power spectrum value at each frequency is divided by the product

of the values of the two power spectra at that frequency to produce the squared coherency spectrum, $K(f_i)$. Its mathematical form is given in Equation A2.6 of Appendix 2. As the expression shows, this normalisation would yield a value of 1 for all frequencies, because the numerator equals the denominator.

To avoid the coherency spectrum having a value of 1 at each frequency, each spectrum is smoothed before the calculation of the coherency spectrum values. The smoothing has the effect of removing high-frequency fluctuations on the spectrum, and broadens the peaks of each spectrum. At some of the frequencies, this broadening increases the value of the normalising function (see the denominator of Equation A2.6 of the Appendix 2) and causes the value of the resulting coherency spectrum to be less than 1.

Interpretation of the correlation of data with the use of a coherency spectrum should be carried out with caution, because:

- The values of the coherency spectrum depend on the amount of smoothing applied; and
- A low value of coherency at a given frequency may be caused by the absence of power in the original power spectra.

2.3.4 Power coherency number

To summarise the variation of power coherency for different station separations, a power coherency number, C is produced for each station separation at each site in the following manner. At a number of frequencies within a given range, the cross-power spectrum value is multiplied by the corresponding value of the coherency spectrum and the resultant products are summed. The value of C is obtained by dividing the summed products by the sum of the amplitudes of the cross spectrum at each of the frequencies. The mathematical expression for C is given in

Equation A2.7 of the Appendix 2. Values of C lie between 0 and 1. A value of C near 1 implies that there is high power coherency over the complete range of frequencies for which it has been calculated. A low value of C indicates that at some frequencies in this range there is a lack of coherent power detected by the two receivers.

A value of C may be used to indicate the power coherency between two time series measured for the same component (e.g., the Z component) at two separated stations, or between two time series measured for any two components (e.g., the X and Z components) at the same station.

2.4 Results of high-frequency sferics correlation measurements

2.4.1 Field sites

Measurements of the correlation of the three components of sferics noise have been made at four sites in Australia (Figure 2.2): at Ku-Ring-Gai National Park near Sydney, NSW, at various mineral exploration areas near Mt Isa, Queensland, near Koolpinyah, east of Darwin, NT, and near Parkes, NSW. High-frequency (> 5 kHz) sferics have been measured at all these sites, and low-frequency measurements have been made at Ku-Ring-Gai National Park and near Darwin. Table 2.2 summarises the main receiver configurations used at each site.

At Ku-Ring-Gai National Park, correlation measurements were made with receiver separations of 0, 230, 500, 750 and 1000 m.

Near Mt Isa, measurements were made at an area with homogeneous conductivity (Moondara) with 500 and 1000 m separations, at an area with heterogeneous conductivity (near the Hilton Mine) with separations of 510 and 900 m, and at an area (Native Bee) with a magnetic anomaly between the two

Table 2.2 Details of sites at which sferics correlation measurements have been made.

Site	Area	Receiver separation
Ku-Ring-Gai Park (High frequency: February-March, 1994; Low frequency: August, 1994)	West Head Road	0, 230, 500, 750 and 1000 m
Mt Isa (March, 1994)	Moondara (homogeneous conductivity)	500 and 1000 m
	Hilton Mine (heterogeneous conductivity)	510 and 900 m
	Quartzite cliffs (highly resistive)	25 and 70 m vertical separation
	Native Bee (magnetic anomaly)	500 m
Koolpinyah, near Darwin (December, 1994)	Gunn Point Road	0, 1, 5 and 11 km
	Beach-inland	8.9 km
	Beach-beach	6.4 km
Parkes (August, 1995)	Mineral prospect	2 and 4 km

receivers separated by 500 m. In addition, correlation measurements were made with two receivers separated vertically by 25 and 70 m on highly-resistive quartzite cliffs.

Correlation measurements were made northeast of Darwin at Koolpinyah. Along the Gunn Point road, the measurements were made with receiver separations of 0, 1, 5 and 11 km, using GPS one-second timing pulses to synchronise the receivers. Measurements were also made with at least one receiver placed near the sea. In one set of these measurements, the second receiver was placed at a distance of 8.9 km inland from the beach, while in the other set of measurements, both receivers were placed on the beach at a distance of 6.4 km from each other.

At Parkes, correlation measurements were made with receiver separations of 2 and 4 km. These measurements are explained in detail in Section 7.2 of Chapter 7.

2.4.2 Plots of sferics time series and correlation functions

To enable an initial inspection of the degree of correlation between sferics measured at two stations with a given separation, a number of blocks of data were chosen and the time series measured at both stations were plotted together with various functions indicating the correlation between the two series. The same format is used for each plot. Plots of the time series measured at each station are followed by the cross-correlation function of these two time series, the cross-power spectrum, the cross-phase spectrum and the squared coherency spectrum. This procedure has been carried out for all station separations at all the sites at which sferics measurements have been made.

Examples of sferics data plots are given in Figures 2.4, 2.5 and 2.6, which show the time series and correlation functions for the X, Y and Z components, respectively, of high-frequency sferics data recorded in December 1994 at a station separation of 11 km at Koolpinyah, near Darwin. This is the maximum separation at

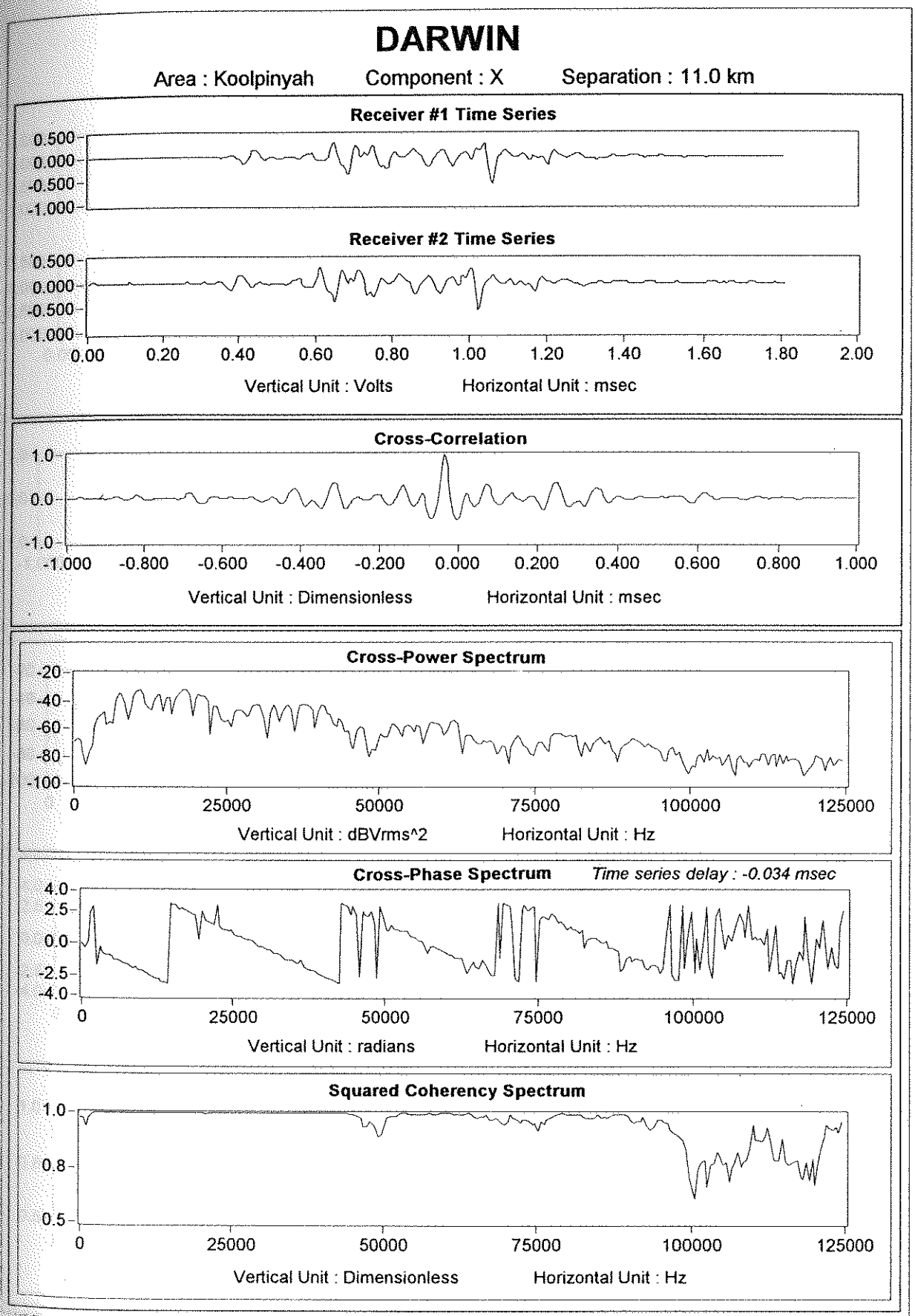

Figure 2.4 Example of time series, correlation function, and cross-power and phase spectra for the X component of high-frequency sferics data recorded in December 1994 at a station separation of 11 km at Koolpinyah, near Darwin.

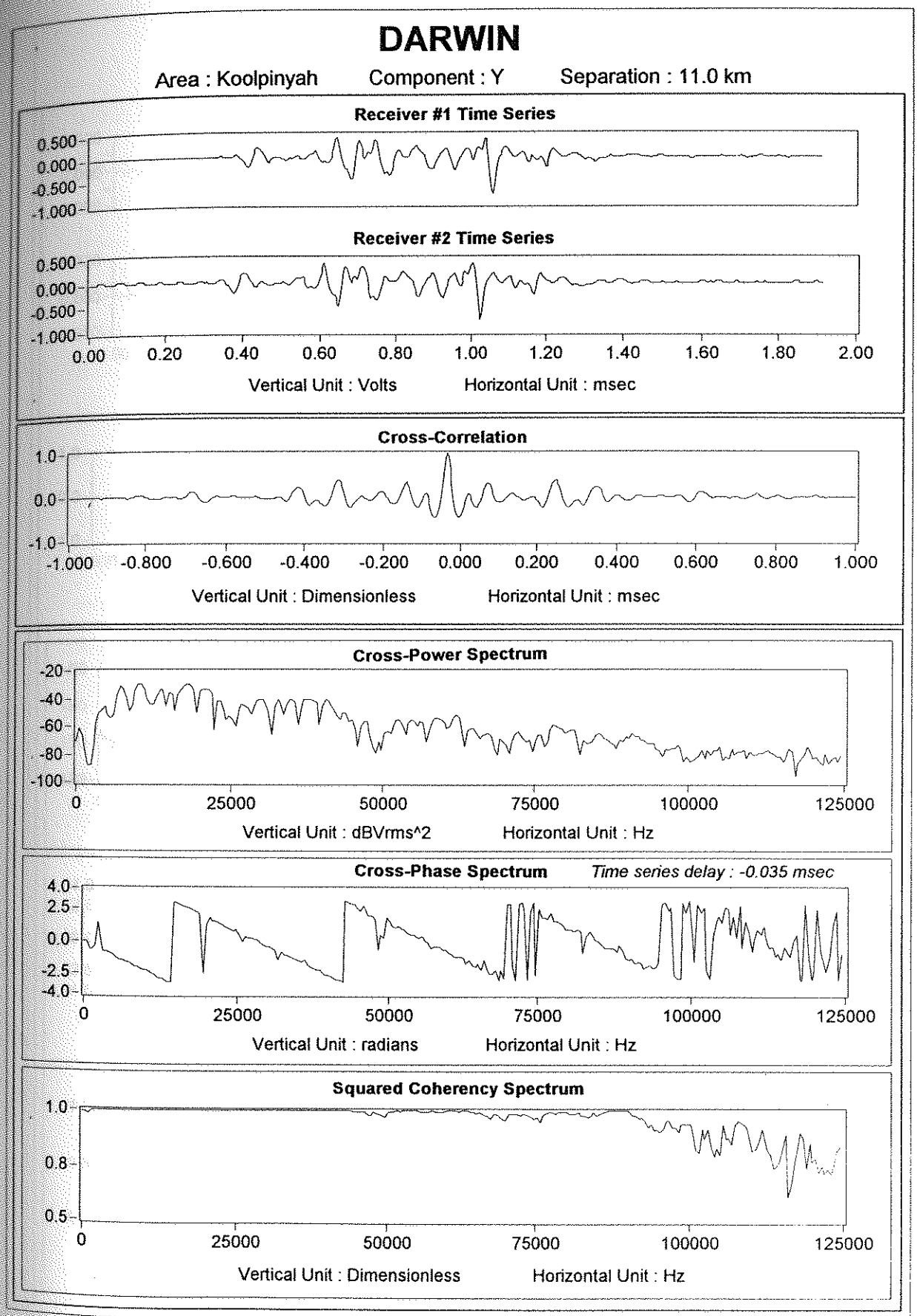

Figure 2.5 Example of time series, correlation function, and cross-power and phase spectra for the Y component of high-frequency sferics data recorded in December 1994 at a station separation of 11 km at Koolpinyah, near Darwin.

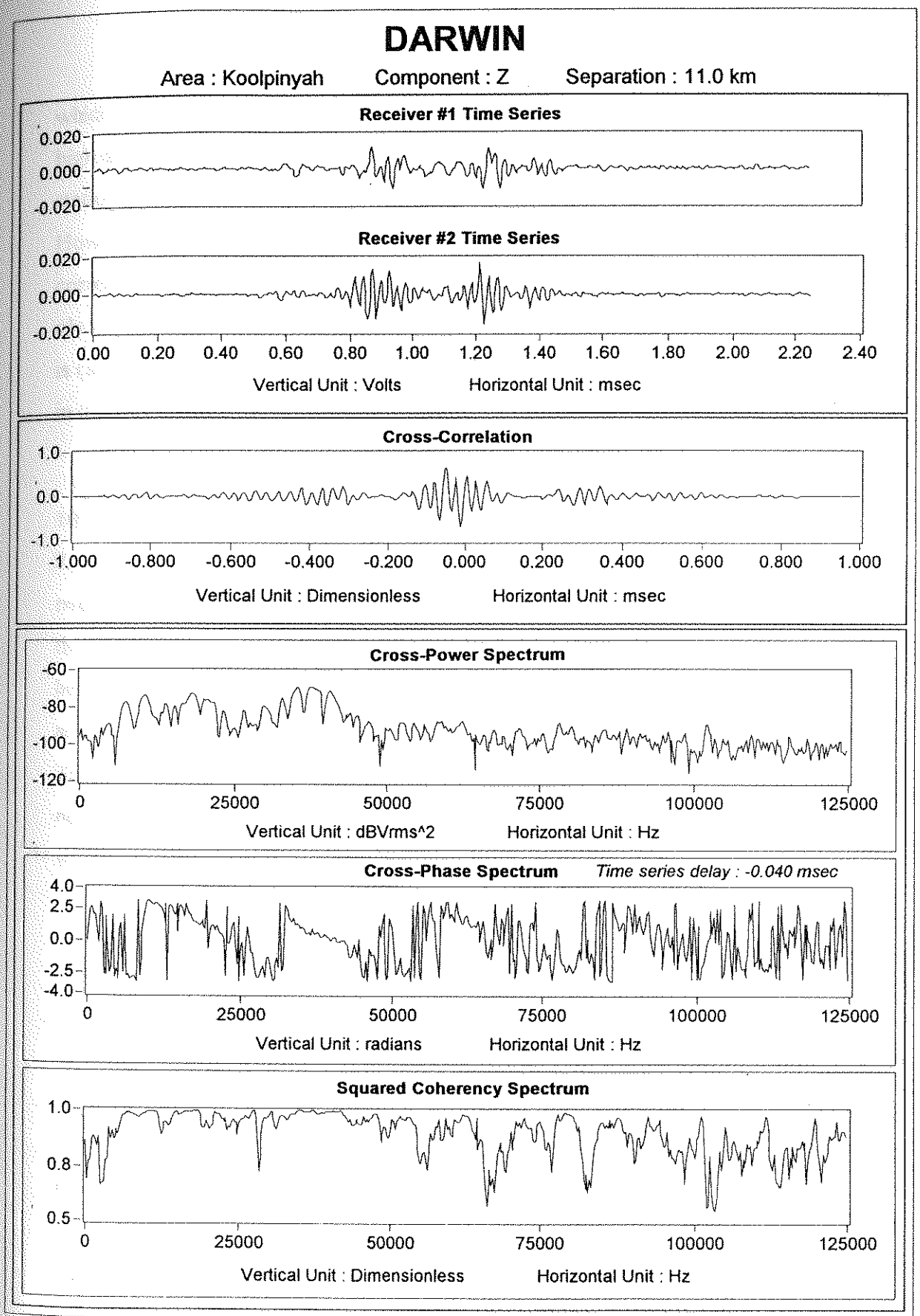

Figure 2.6 Example of time series, correlation function, and cross-power and phase spectra for the Z component of high-frequency sferics data recorded in December 1994 at a station separation of 11 km at Koolpinyah, near Darwin.

which sferics correlation measurements have been made, and the results indicate a high degree of correlation for the X and Y components of the sferics, even at this station separation. The correlation coefficient for these two components is 1.0. However, the correlation coefficient for the Z component is less (~ 0.6), and the correlation function is more complex (see Figure 2.6) than the correlation function obtained for the X and Y components. As mentioned in Section 2.3.2, this complexity is caused by the presence of relatively high VLF noise occurring with the sferics noise in the Z component measurements.

The cross-power spectra show coherent frequency components of up to about 100 kHz in the X and Y components. Coherent power is observed up to 50 kHz in the Z component of the sferics noise. Coherence in the Z component power is observed over a narrower frequency range because the bandwidth of the Z-component coil of the RVR is lower than the bandwidth of the X- and Y-component coils, and also because in this case, the maximum amplitude of the Z-component sferics is a factor of at least 30 lower than the maximum amplitude of either the X or Y component sferics. The squared coherency spectra reflect this behaviour, and show values of 1.0 up to nearly 100 kHz for the X and Y components (Figures 2.4 and 2.5), and become noisy with values less than 1.0 above 50 kHz for the Z component (Figure 2.6).

The slope of the cross-phase spectra gives a time shift between the two time series of -34 μs for the X component and -35 μs for the Y component. By convention, a positive sign for the delay indicates that the receiver at position denoted #2 detects the corresponding sferics pulse after receiver denoted #1. In this case then, the sferics wavefront reaches receiver #2 first. Also, the wavefront must be travelling in a direction parallel to the line joining the two receivers, since a wavefront travelling at the speed of light will traverse 1 km in 3 μs, and the maximum delay expected between corresponding sferics pulses is 33 μs for a station separation of 11 km. A value of the time shift, greater than this maximum, reflects the amount of error in its

measurement. For example, the time shift of -40 μs obtained from the Z component has an error larger than the time shift obtained from the X or Y component, because the spectrum from which it is derived is noisy (Figure 2.6).

2.4.3 Power coherency numbers for two-station measurements

The power coherency number, C defined by Equation A2.7 in the Appendix 2 has been calculated for all areas at Ku-Ring-Gai National Park, Mt Isa and Koolpinyah. The values are presented in Table 2.3 for the X, Y and Z components of the sferics measured at the two stations with separations as shown in the table. The standard error shown for each value was obtained by calculating a value of C using at least 20 separate sferics pulses. It can be seen that in all cases the standard error does not exceed 0.01. The values of C show a high power coherency for all the components at all separations, including the maximum separation of 11 km at Koolpinyah. These values therefore indicate that high-frequency sferics noise should be eliminated effectively with filters based on the prediction of high frequency sferics noise. The performance of such filters is examined in more detail in Chapters 5 and 7.

2.4.4 Power coherency numbers for two components of sferics

Table 2.4 shows values of C obtained for the X and Y components, the Z and X components and the Z and Y components of sferics pulses measured at single stations as shown in the table. A high level of amplitude coherence is observed for all combinations of two components, with values of C ranging from 0.89 to 0.93 for the X-Y combination, 0.85 to 0.90 for the Z-X combination, and 0.84 to 0.90 for the Z-Y combination. A filter based on the prediction of the Z component from the X and Y components (i.e., a local noise prediction filter) would therefore be expected to reduce the Z component of sferics noise effectively. A local noise prediction filter is explained in more detail in Chapter 4.

Table 2.3 **Coherency numbers calculated for the X, Y, and Z components of sferics pulses recorded at two stations with separations as shown.**

Site	Area	Receiver Separation	Coherency Number		
			X	Y	Z
Ku-Ring-Gai Park	West Head Road	500 m	0.98±0.01	0.98±0.01	0.86±0.00
		1000 m	0.91±0.01	0.95±0.01	0.92±0.01
Mt. Isa	Moondara	500 m	0.97±0.00	0.88±0.00	0.86±0.01
		1000 m	0.92±0.01	0.86±0.00	0.85±0.00
	Hilton Mine	510 m	0.97±0.00	0.94±0.01	0.84±0.00
		900 m	0.94±0.01	0.87±0.01	0.82±0.01
	Quartzite Cliffs	25 m	0.98±0.01	0.97±0.01	0.91±0.00
		70 m	0.92±0.01	0.85±0.00	0.87±0.01
	Native Bee	500 m	0.93±0.00	0.93±0.01	0.86±0.01
Koolpinyah	Gunn Point Road	5 km	0.90±0.01	0.91±0.01	0.84±0.01
	Gunn Point Road	11 km	0.93±0.00	0.94±0.00	0.85±0.01
	Beach-inland	8.9 km	0.92±0.01	0.92±0.01	0.85±0.01
	Beach-beach	6.4 km	0.92±0.01	0.89±0.01	0.84±0.01

Table 2.4 Coherency numbers calculated for X and Y components, Z and X components, and Z and Y components of sferics pulses recorded at single stations as shown.

Site	Area		Coherency Number		
			XY	ZX	ZY
Ku-Ring-Gai Park	West Head Road	Base station	0.93±0.01	0.90±0.01	0.90±0.01
		500 m from base station	0.93±0.01	0.90±0.01	0.89±0.01
		1 km from base station	0.92±0.01	0.90±0.01	0.87±0.01
Koolpinyah	Gunn Point Road	Base station	0.91±0.01	0.85±0.01	0.86±0.01
		5 km from base station	0.91±0.01	0.88±0.01	0.89±0.01
		11 km from base station	0.91±0.01	0.86±0.01	0.87±0.01
	Beach	8.9 km from inland base station	0.93±0.01	0.88±0.00	0.88±0.00
		Beach base station	0.89±0.01	0.88±0.01	0.86±0.01
		6.4 km from beach base station	0.90±0.01	0.89±0.01	0.84±0.01

2.4.5 Effect of ground conductivity on high-frequency sferics

To examine the effect of different ground conductivity at the two stations at which simultaneous measurements of high-frequency sferics were made, the ratio of the root-mean-square amplitude of sferics measured at the two stations was calculated. The results are shown in Table 2.5 for the X, Y and Z components of sferics measured with various receiver separations at the Ku-Ring-Gai National Park and Koolpinyah sites. A standard error calculated from at least 20 sferics pulses is shown for each value of C.

The table includes values for zero separation of the receivers at the two sites. In this case, the ratio of the amplitude for all components is 1.0 within experimental error, as expected. For the other separations, the ratios are almost 1.0 for the X and Y components. The greatest effect is seen on the Z component, where the lowest ratio of 0.72 ± 0.06 is obtained for the 8.9 km separation at Koolpinyah. It is expected that generally the Z component will be the most affected by a difference in ground conductivity at the two stations, as it couples more readily with a horizontally-layered ground.

2.5 Results of low-frequency sferics measurements

Three-component low-frequency sferics measurements have been made with a 1 kHz low-pass filter at the output of the signal preamplifiers and with a sampling frequency of 10 kHz. The vertical component was measured with a two-turn square loop with sides of 100 m, and the two horizontal components were each measured with an induction coil (Drover) with a passive area of 500 m^2, which was constructed specifically with high sensitivity to detect the horizontal components of low-frequency sferics noise.

Table 2.5 The ratio of root-mean-square amplitudes of sferics calculated for the X, Y, and Z components of sferics pulses recorded at two stations with separations as shown.

Site	Area	Receiver Separation (km)	Amplitude Ratio		
			X	Y	Z
Ku-Ring-Gai Park	West Head Road	0.0	1.02±0.00	1.02±0.01	1.33±0.04
		0.5	1.08±0.01	1.37±0.04	0.89±0.11
		1.0	0.97±0.03	1.38±0.12	0.88±0.02
Koolpinyah	Gunn Point Road	0.0	1.06±0.01	1.00±0.00	1.14±0.02
	Gunn Point Road	5.0	1.07±0.03	1.02±0.02	0.99±0.08
	Gunn Point Road	11.0	0.97±0.01	1.05±0.01	0.75±0.05
	Beach-inland	8.9	1.04±0.01	1.06±0.01	0.72±0.06
	Beach-beach	6.4	0.99±0.01	0.96±0.02	0.77±0.08

The occurrence of a sferics pulse is identified by the short (~ 1 ms) impulse response of the 1 kHz filter. In order to investigate the validity of sferics spectra measured at frequencies below 1 kHz using 1 kHz lowpass filter, simultaneous broadband (<100 kHz) and narrowband (10 Hz to 1 kHz) measurements of time series of sferics noise have been made. In both cases, an ADC sample rate of 250 kHz was used to digitise each component of the noise. In addition, simultaneous sferics measurements were made with an RVR-3C and a Drover. Separated coils are used to detect the X and Y components. For either type of sensor, the component of the noise being discussed follows the name of the sensor. Thus, DRVR-Z refers to the Z component of the sferics noise measured with a Drover.

2.5.1 Comparison of simultaneous DRVR and RVR-X broadband measurements

Figures 2.7 and 2.8 compare the DRVR-X and RVR-X power spectra obtained for sferics noise measured simultaneously over a one-second time period. Both spectra have been derived from broadband measurements, and are plotted solely for the frequency range of 0 to 1 kHz. To show the contribution of sferics noise, on each spectrum there is a plot of background noise obtained from time series recorded during periods of low sferics activity. Clearly, the DRVR detects noise above the background level, but the RVR has less sensitivity and sferics power is almost at background level for this case.

Figures 2.9 and 2.10 present low-frequency sferics spectra obtained from simultaneous broadband DRVR-Z and RVR-Z measurements. The Z (vertical) component is expected to be about a factor of 10 lower than the X or Y component. In this case, sferics noise is not significantly greater than the background level for either the RVR or DRVR, and a sensor with larger area (e.g., a 100 m square loop) needs to be used to detect sferics power in this frequency range.

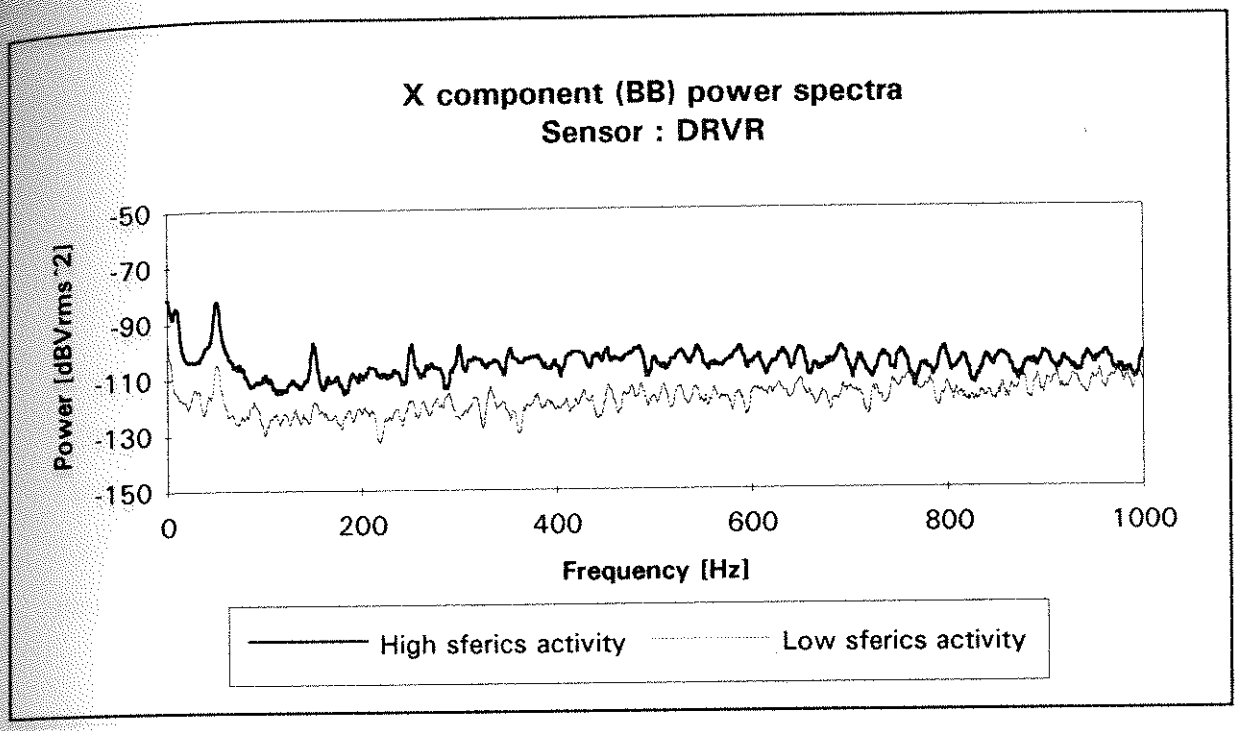

Figure 2.7 Power spectra of the broadband X-component time series measured with a DRVR during periods of high and low sferics activity.

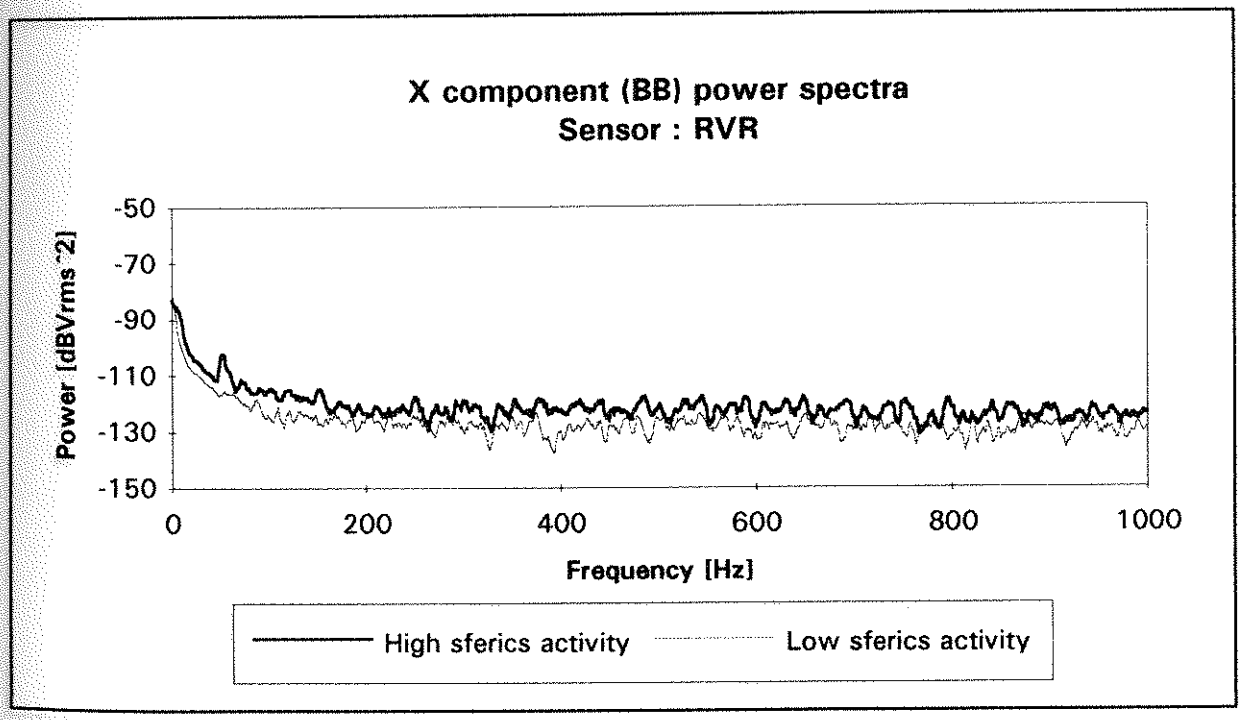

Figure 2.8 Power spectra of the broadband X-component time series measured with an RVR-3C during periods of high and low sferics activity. These power spectra were obtained from a one-second time period of time series measured simultaneously with that of Figure 2.7.

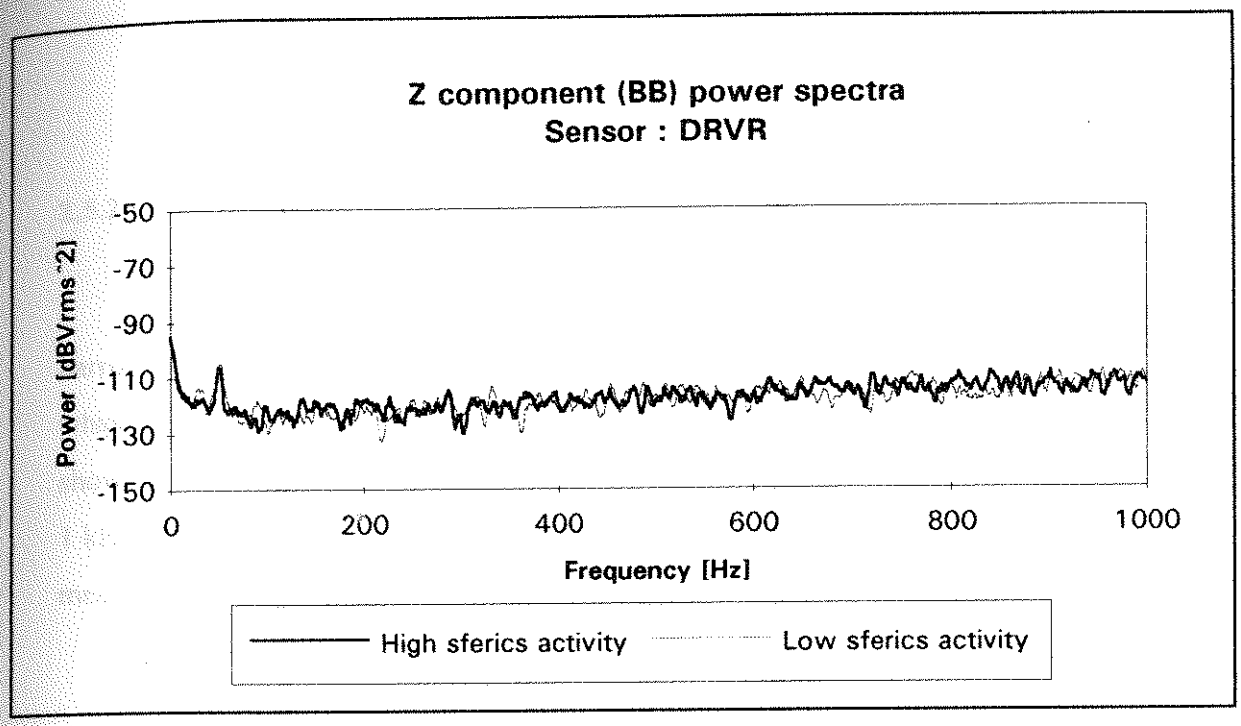

Figure 2.9 Power spectra of the broadband Z-component time series measured with a DRVR during periods of high and low sferics activity.

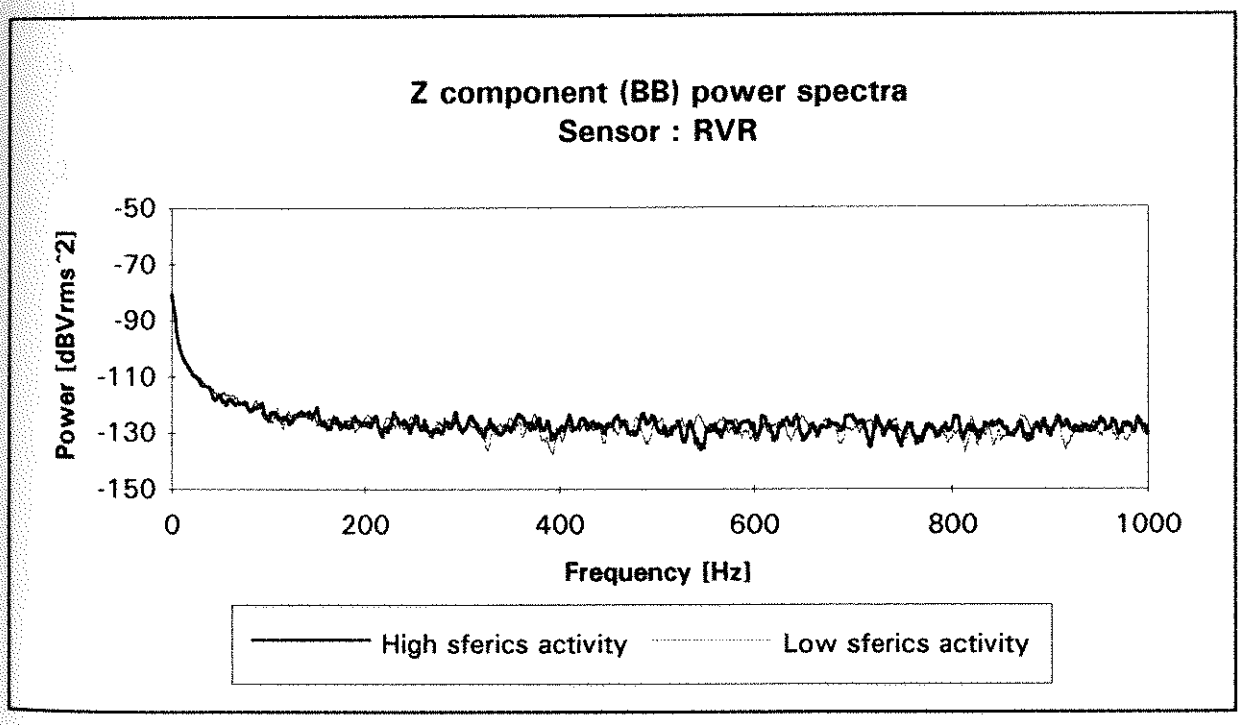

Figure 2.10 Power spectra of the broadband Z-component time series measured with an RVR-3C during periods of high and low sferics activity. These power spectra were obtained from a one-second time period of time series measured simultaneously with that of Figure 2.9.

2.5.2 Comparison of simultaneous broadband and narrowband measurements

Figure 2.11 shows the DRVR-X power spectrum obtained from the narrowband time series measured simultaneously with the broadband time series for which the power spectrum is presented in Figure 2.7. A comparison of these two plots shows that both measurements yield similar spectra. Thus, any response from the 1 kHz filter does not contribute significantly to the power spectrum of the time series measured with this filter present.

Figure 2.12 presents the DRVR-Z power spectrum for sferics noise measured with a 1 kHz filter present. The corresponding spectrum obtained from simultaneous broadband DRVR-Z sferics measurements is shown in Figure 2.9. The two spectra are similar. In the same manner, the narrowband spectra for RVR-X and RVR-Z (Figures 2.13 and 2.14) show no significant differences from the corresponding broadband spectra (Figures 2.8 and 2.10).

2.5.3 Comparison of DRVR-X spectra with previously-published results

To compare the measured low-frequency spectra with results published in the literature, the power of each spectrum was converted to units of magnetic field strength, B, in units of nT/$\sqrt{\text{Hz}}$. Figure 2.15 shows an example of the spectra of the X component measured below 1 kHz for one-second block of sferics data recorded in Darwin in summer and a block of data recorded at Ku-Ring-Gai National Park in autumn. The sferics count rates of Darwin and Ku-Ring-Gai data are 183 and 22 pulses per sec, respectively. The method of obtaining sferics count rates was explained in Section 2.2 of this chapter. The results are compared with a spectrum of average sferics activity published by Macnae et al. (1984) as well as a spectrum of

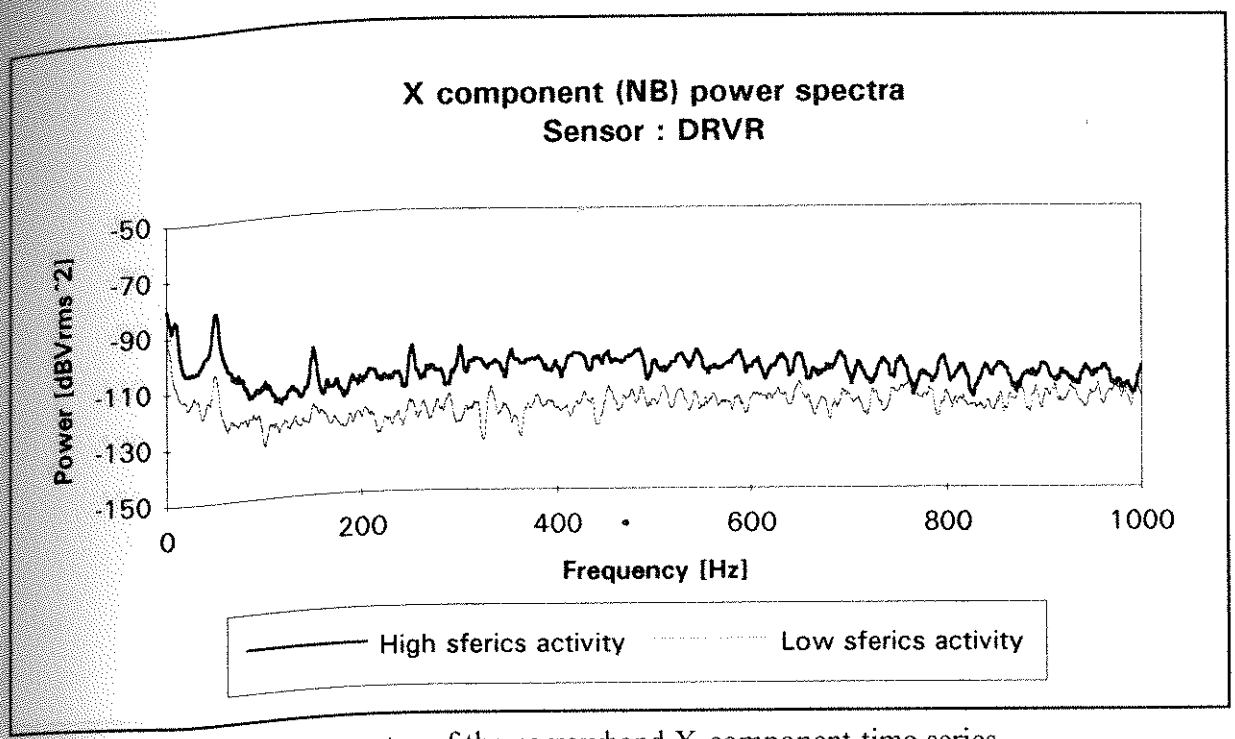

Figure 2.11 Power spectra of the narrowband X-component time series measured with a DRVR during periods of high and low sferics activity. These power spectra were obtained from a one-second time period of time series measured simultaneously with that of Figure 2.7.

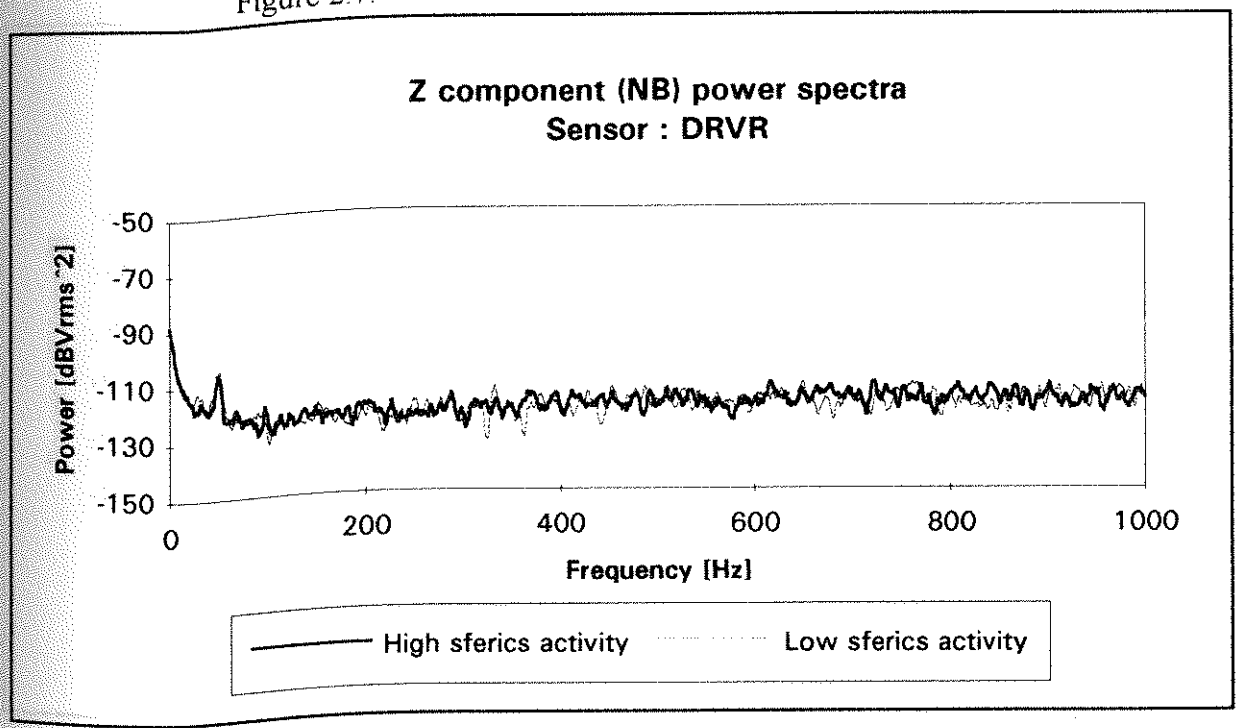

Figure 2.12 Power spectra of the narrowband Z-component time series measured with a DRVR during periods of high and low sferics activity. These power spectra were obtained from a one-second time period of time series measured simultaneously with that of Figure 2.9.

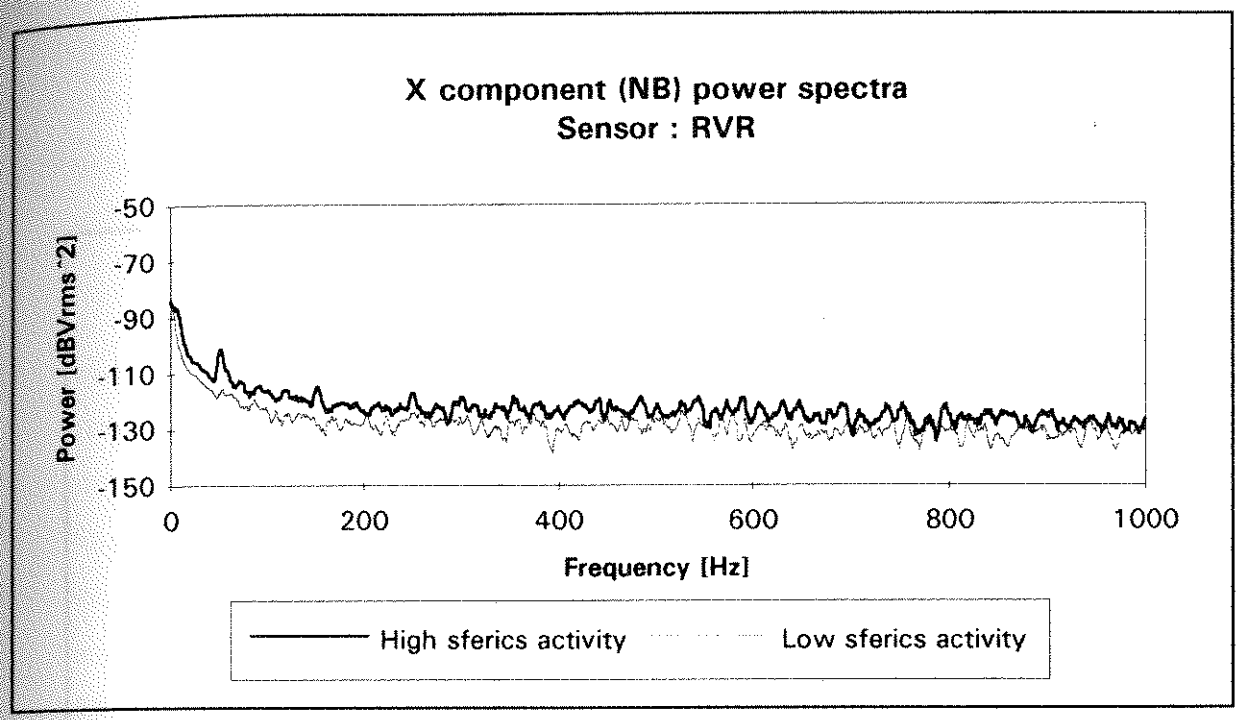

Figure 2.13 Power spectra of the narrowband X-component time series measured with an RVR-3C during periods of high and low sferics activity. These power spectra were obtained from a one-second time period of time series measured simultaneously with that of Figure 2.8.

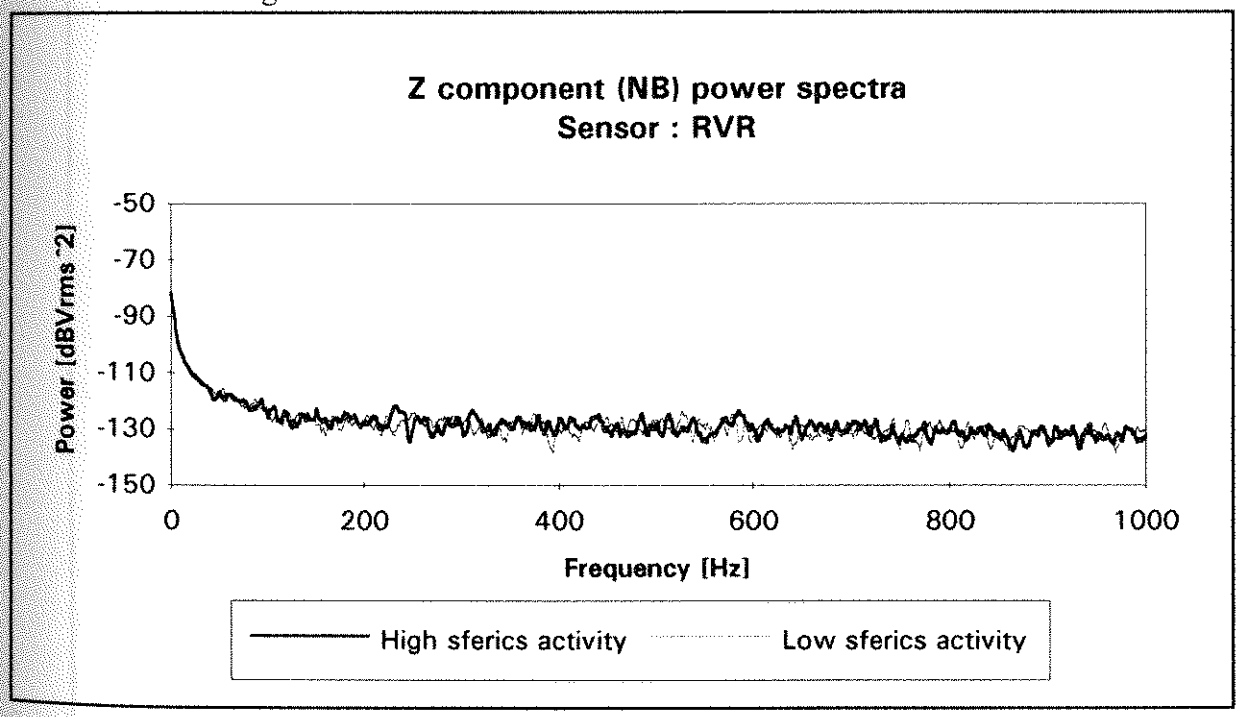

Figure 2.14 Power spectra of the narrowband Z-component time series measured with a DRVR during periods of high and low sferics activity. These power spectra were obtained from a one-second time period of time series measured simultaneously with that of Figure 2.10.

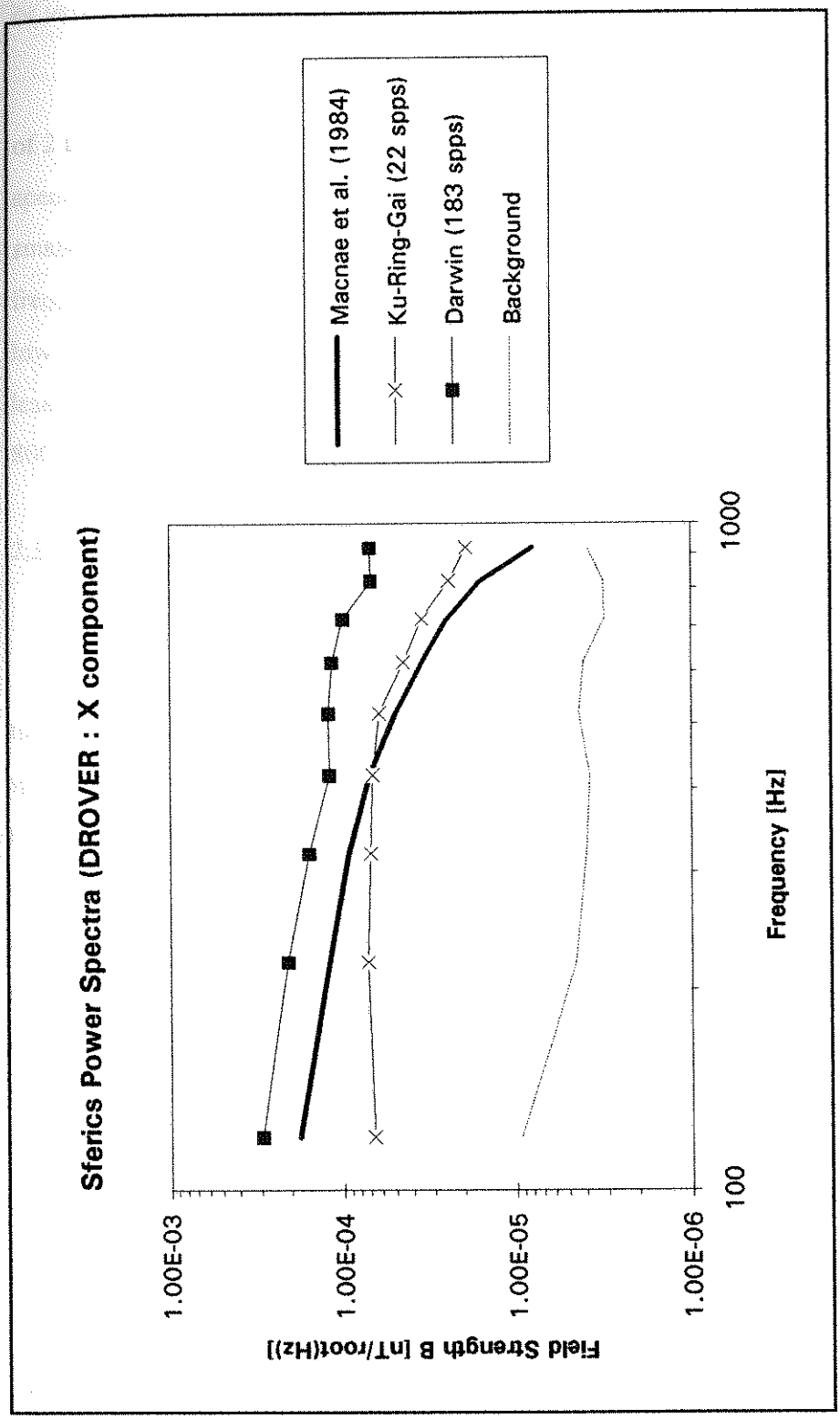

Figure 2.15 Comparison of the spectra of the measured X-component of sferics noise below 1 kHz with a spectrum of average sferics activity published by Macnae et al. (1984).

background EM noise measured at Ku-Ring-Gai National Park during a period of no or very low sferics activity.

The results show that the amplitudes in summer near Darwin may be a factor of 2 to 3 larger than the spectrum of Macnae et al. (1984). The low-frequency spectrum measured in autumn in Ku-Ring-Gai National Park is a factor of 2 to 5 smaller in the frequency range of 100 to 300 Hz and a factor of 2 higher in the frequency range of 500 Hz to 1 kHz than the Macnae spectrum. The two spectra of low-frequency sferics measured in Darwin and Ku-Ring-Gain National Park are at least an order of magnitude higher than background level at frequencies of 100 to 800 Hz.

2.5.4 Results from measurements of the vertical component of low-frequency sferics

The vertical component of low-frequency sferics was not detected with a one-turn or two-turn 100 m square loop. Figure 2.16 shows a detectable sferics noise spectrum with a 100 m square loop compared with the 12-bit ADC noise spectra for three different preamplifier gains of 1, 10, and 100 in a frequency range of 100 Hz to 1 kHz. Since the vertical component of the sferics noise is a factor of about 10 lower than the horizontal component, sferics noise (denoted as the bold line-solid square shown in Figure 2.16 were calculated from values given by Macnae et al. (1984) shown in Figure 2.15. It is seen that the ADC noise with a preamplifier gain of 1 is a factor of at least 30 greater than the sferics noise at a frequency of 100 Hz. The ADC noise even with a preamplifier gain of 10 is still a factor of three higher than the sferics at a frequency of 100 Hz. Therefore, for Z component measurements of low-frequency sferics, a preamplifier gain of at least 100 should be used. However, Z-component sferics greater than 50 mV, which can be measured with an RVR-3C, will saturate the present preamplifier used for sferics measurements.

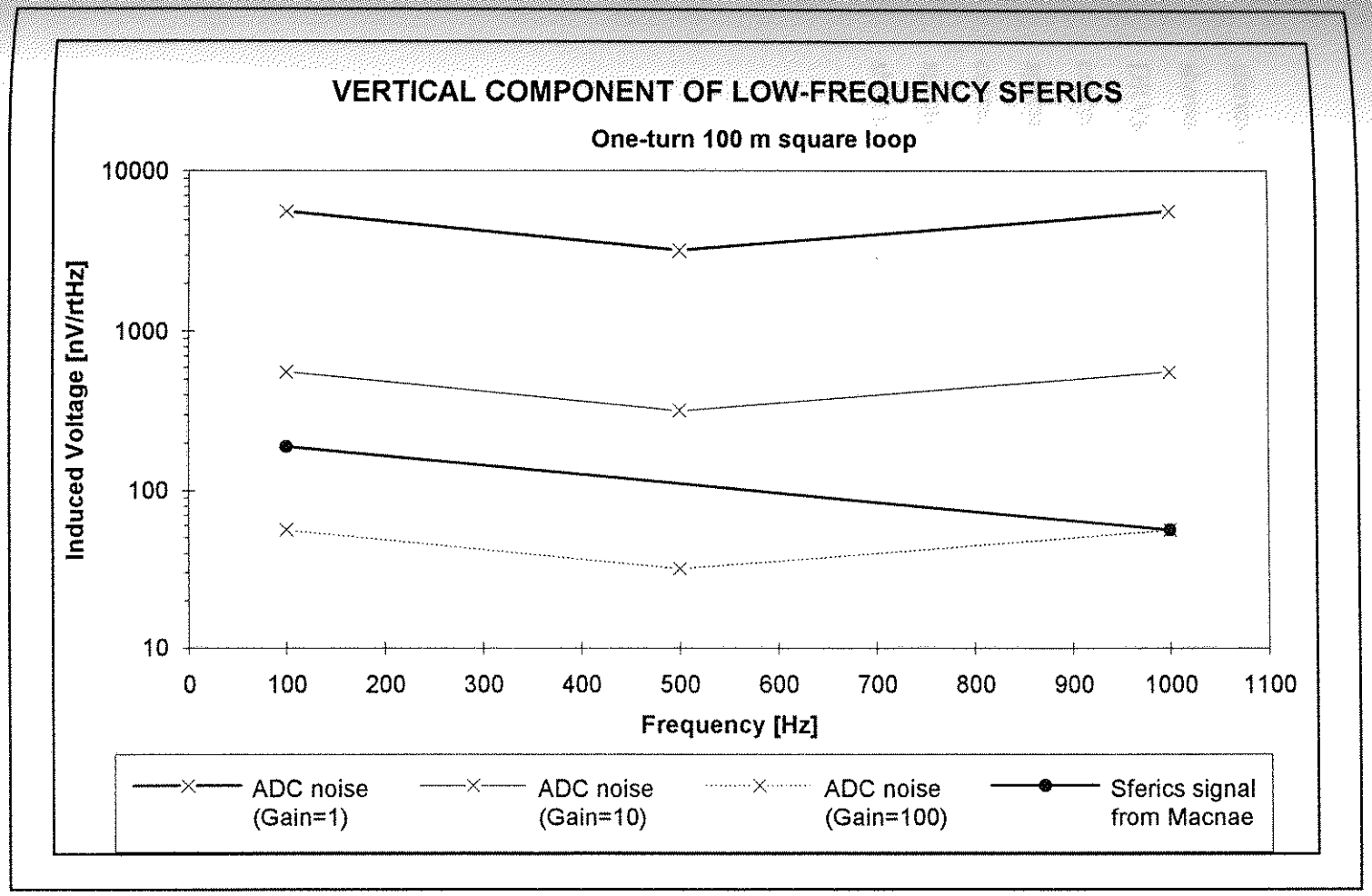

Figure 2.16 Comparison of the spectra of the 12-bit analogue-to-digital converter (ADC) noise with different preamplifier gains of 1, 10, and 100 with a spectrum of average sferics activity published by Macnae et al. (1984).

2.5.5 Correlation of the horizontal components of low-frequency sferics

As an indication of the degree of correlation of low-frequency components of sferics noise, an example of simultaneous narrowband measurements of sferics noise is shown in Figure 2.17 for the X component of sferics noise measured with two DRVRs separated by a distance of 11 km at Koolpinyah, near Darwin. The cross-correlation function has a value of 0.9 at a time shift of zero. The cross-power spectrum shows a high level of correlation at all frequencies below 1 kHz, since no correlation would be at a level of approximately -105 dBV^2. The cross-phase spectrum has zero slope and therefore, demonstrates that there is no measurable time shift between the time series measured with the two separated receivers.

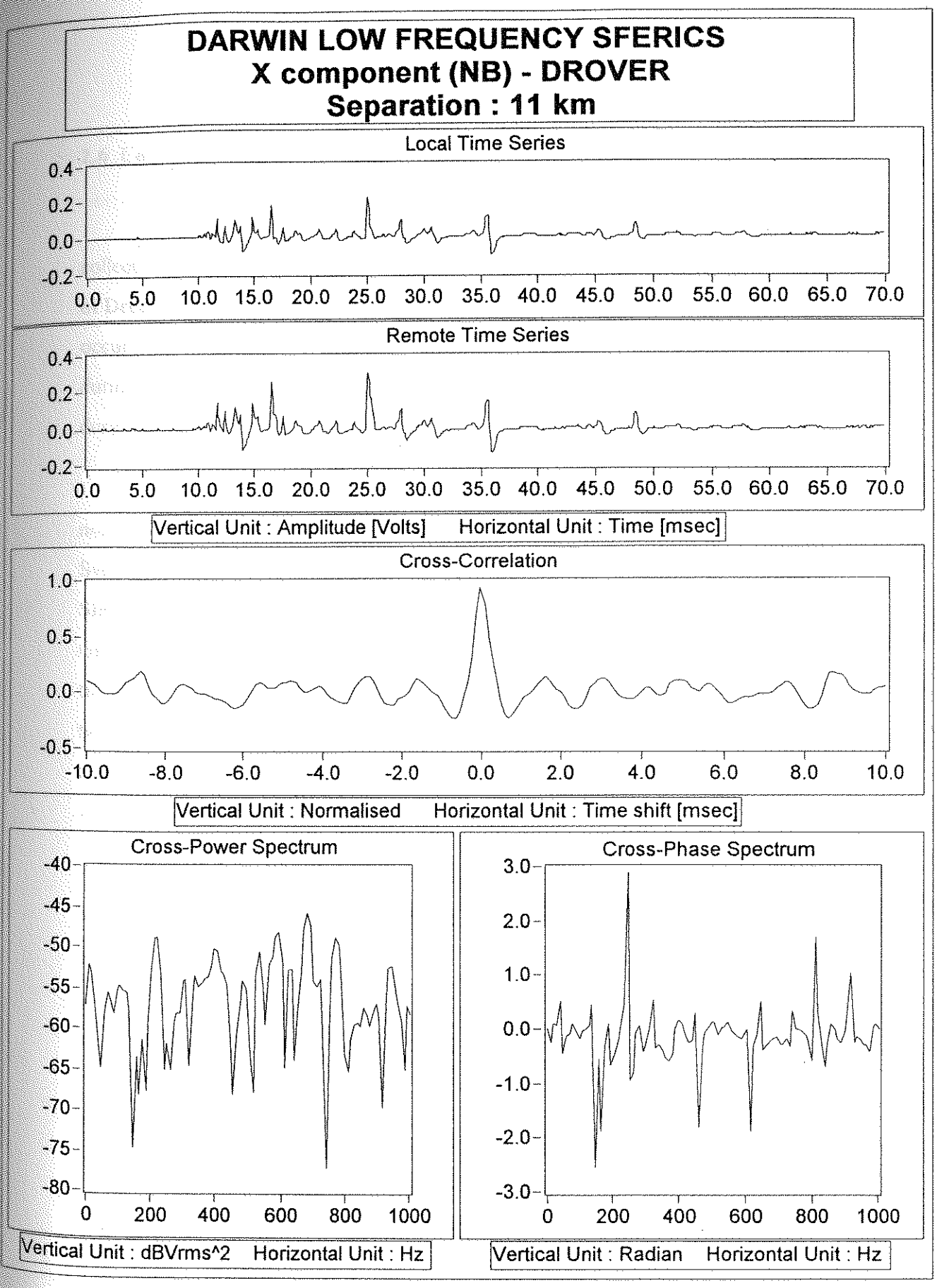

Figure 2.17 Example of time series, correlation function, and cross-power and cross-phase spectra for the X component of low-frequency (below 1 kHz) sferics data recorded in December 1994 at a station separation of 11 km at Koolpinyah, near Darwin.

2.6 Conclusion

To investigate the daily variation of sferics activity, sferics noise data were collected at Ku-Ring-Gai National Park from 11:00 AM of 28th to 11:00 AM of 29th of December 1994 with an interval of 30 min. The minimum sferics activity periods occur from 6:30 AM to 1:30 PM and from 6:30 to 10:30 PM. The sferics count rates during these minimum activity periods are about 3 to 9 times smaller than those during periods of maximum sferics activity.

Three-component measurements of the correlation of high-frequency sferics noise at frequencies above 5 kHz have been made at Ku-Ring-Gai National Park near Sydney, at mineral exploration areas near Mt Isa, at Darwin, and at Parkes using SIROTEM receiver coils (RVR-3C) separated by a distance as great as 11 km. Generally, it is found that there is close correlation between the three components of the sferics at a given stations, and between corresponding components measured at two stations separated by distances up to 11 km. The greatest dispersion effect due to a difference in ground conductivity at two separated stations can been seen on the vertical component of sferics noise.

The low-frequency horizontal components of sferics noise can be measured with a Drover coil, which has been specially designed to detect this noise. Below a frequency of 1 kHz, the power spectra of sferics time series measured with this coil are consistent with previously-published results. A 1 kHz anti-aliasing filter does not significantly alter the spectrum of sferics noise below 1 kHz. For simultaneous measurements with two separated receivers, a high degree of correlation is obtained for the horizontal (X) component of low-frequency sferics noise even when the receivers are separated by a distance of 11 km.

A large loop did not detect sferics below 1 kHz, even when a two-turn 100 m square loop was used, since the 12-bit ADC noise level with preamplifier gains of 1 and 10 is greater than the detectable sferics noise.

It is conclude that there is high correlation between corresponding horizontal components of low-frequency sferics noise measured at two stations separated distances up to 11 km. The cross-phase spectrum has zero slope and therefore, demonstrates that there is no measurable time shift between the time series measured with two separated receivers. In essence, the speed of light time delays of say 30 μs over 10 km can be insignificant phase shifts at frequencies much below 1 kHz.